

UAV 3D Trajectory Planning Based on Improved A* Algorithm and Differential Evolution

Li Yang*

Department of information engineering
Sichuan Vocational and Technical College of Communications
Chengdu 611130, P. R. China
13568851057@163.com

Liang Tan*

Thai-Chinese International College
Assumption University of Thailand
Bangkok 100027, Thailand
lidorr@sohu.com

Fuquan Zhang

College of Computer and Control Engineering
Minjiang University
Fuzhou, 350108, P. R. China
zhangqing94@126.com

*Corresponding author: Li Yang

Received February 21, 2023, revised March 24, 2023, accepted May 20, 2023.

ABSTRACT. *Track planning technology, as a key technology for UAV mission planning, has always been a major research hotspot in the field of UAVs. In real-life applications, due to the complex and constrained UAV flight environment, how to establish an accurate environment model and how to select an efficient planning algorithm become the elements to solve the trajectory planning problem. In this work, after studying existing trajectory planning algorithms, a method using a combination of improved A* algorithm and differential evolution algorithm is proposed for 3D trajectory planning in complex environments. Firstly, the mathematical modelling of the UAV track planning related problems, including the UAV model, manoeuvrability constraints and equivalent digital maps, is carried out. Secondly, an improved sparse A* algorithm is proposed for solving the winding path problem of the sparse A* algorithm, which reduces the winding path of the trajectory by extracting path feature points and quadratic optimisation. Finally, the improved sparse A* algorithm is combined with the differential evolutionary algorithm and applied to the UAV real-time trajectory planning, where the improved sparse A* algorithm is used for the UAV global trajectory planning and the differential evolutionary algorithm is applied to the emergent threat avoidance, i.e. local trajectory planning. The results of MATLAB simulations show that the proposed method can solve the path-around problem of the sparse A* algorithm and can be flexible in complex environments to achieve dynamic trajectory planning, thus effectively guaranteeing the flight safety of UAVs in practical environments.*

Keywords: Unmanned aircraft; Real-time track planning; 3D maps; A* algorithm; Differential evolution

1. **Introduction.** With the rapid development of modern technology, the technological progress in the field of modern aviation has been strongly advanced. Unmanned Aerial Vehicle (UAV) [1,2,3] is a kind of unmanned aerial vehicle with autonomous control and power drive. The improvement of aerial vehicle technology has led to the gradual application of UAVs.

Drones have the advantages of being small, simple, inexpensive to use, easy to manoeuvre and can work in dangerous environments [4]. UAVs have shown extremely high military value on the battlefield, and thus they will certainly become the main force on the international battlefield in the future. In addition, UAVs are also widely used in civil fields such as disaster prevention and relief, resource and weather detection, and forest fire prevention [5].

However, as the complexity and duration of missions continue to increase, manual handling is no longer sufficient for complex missions. How to make the vehicle with autonomous flight capability is a meaningful research direction. Trajectory planning is the core technology of the UAV Mission Planning System (MPS) [6,7,8]. A good trajectory planning method can help UAVs avoid threats in the battlefield, reduce range and fuel consumption, and improve their survivability and mission success. Trajectory planning techniques can also be used in path planning for civil aviation, cruise missiles, robotics, etc. In addition, as the price of UAVs decreases, more and more companies are using them innovatively in their business to improve their services, such as aerial photography and couriers [9,10]. The application of drones is very promising. Therefore, it is of great practical importance to further study the trajectory planning technology and improve the safety and stability of UAV flight, both from the perspective of military needs and from the perspective of commercial and civil needs.

Because of the many uncertainties in the flight environment, making it difficult to obtain the exact parameters of the global environment, traditional static track planning methods are unable to meet the requirements of the current flight requirements of UAVs [11,12,13]. In contrast, static planning methods achieve the best trajectory, but have the disadvantage of long planning times and the inability to avoid emergent threats in a timely manner [14,15]; dynamic planning methods have high real-time performance, but have the disadvantage of prioritising feasible trajectories before considering the optimal trajectory [16,17]. Therefore, in this work, the statically planned trajectory is first used as a reference in the UAV mission planning system, and the trajectory is dynamically modified according to the situation in the actual process to finally achieve efficient avoidance of emergent threats in the flight environment.

1.1. **Related Work.** Route planning is an important branch of research in the field of artificial intelligence, which involves searching for an optimal route from a starting point to a goal point by satisfying some or other optimisation criterion (e.g. least fuel consumption, shortest route, shortest time, safest route, etc.).

Guerrero et al. [18] used a three-dimensional geometric approach to solve the problem of minimum turn radius and target entry direction in path planning, but ignored the threats in the environment and did not apply to threatening environments. However, the threats present in the environment are ignored and are not applicable to threatening environments.

Finding a general algorithm that solves all problems is extremely challenging due to the complexity of the UAV flight environment and the many manoeuvrability constraints. Therefore, the key to trajectory planning under different environments and constraints is to find trajectory planning algorithms with shorter convergence times and more accurate planning results. Arantes et al. [19] used an improved genetic algorithm to achieve

smooth trajectory planning for multiple UAVs, which can be used for forest fire prevention, surveillance, and cruising. Huang et al. [20] used a particle swarm optimisation algorithm to realise track planning. Majeed et al. [21] introduced a variable-step sparse A* algorithm. When a complex environment is encountered, the search step length of the algorithm can be reduced to allow the UAV to pass safely, while improving the search accuracy and robustness. However, under special circumstances, the algorithm may also miss the optimal path and go around, leading to search failure. Chen et al. [22] used an improved artificial potential field method to plan an optimal trajectory for the UAV in a real-time environment, but did not consider the UAV's manoeuvrability constraints and was not suitable for realistic applications.

Due to the large area involved in UAV trajectory planning, traditional search algorithms take a long time to plan an optimal trajectory and have high memory space requirements. In order to increase the search speed and reduce the memory space requirements, the traditional solution is to project the flight environment and reduce it to a 2D flat spatial environment at a certain altitude. The disadvantage of this processing is that it does not fully contain the original terrain information and does not allow for good terrain following and threat avoidance. Based on this factor, this work is a study of UAV trajectory planning in a 3D environment. The study of the trajectory planning problem can generally be divided into two categories [23,24]: one type is static trajectory planning, which refers to the problem where the threats and constraints are all known prior to the trajectory planning, under which the planning is carried out to obtain an optimal trajectory as the UAV reference trajectory. This type of problem does not require high real-time algorithms and has high requirements on the accuracy of the trajectory, which is generally done in advance using ground computers; the other type is real-time trajectory planning, which can also be called dynamic trajectory planning, refers to the threat conditions are partially unknown, and the changes in environmental information are obtained through on-board sensors during the flight, according to which planning is carried out to avoid sudden threats. Dynamic planning requires a high level of real time and does not require high accuracy of the trajectory. The focus of the research in this work is on dynamic planning.

1.2. Motivation and contribution. This work proposes a method using an improved A* algorithm combined with a differential evolutionary algorithm for 3D dynamic trajectory planning in complex environments, following a study of existing trajectory planning algorithms.

The main innovations and contributions of this study are shown as follow:

(1) Mathematical modelling of problems related to UAV trajectory planning, including UAV models, manoeuvrability constraints and equivalent digital maps.

(2) An improved sparse A* algorithm is proposed for solving the winding path problem of the sparse A* algorithm, which reduces the winding path of the trajectory by extracting path feature points and quadratic optimization.

(3) The improved sparse A* and Differential Evolutionary(DE) algorithms are combined and applied to UAV 3D dynamic trajectory planning, where the improved sparse A* algorithm is used for UAV global trajectory planning, while the differential evolutionary algorithm is applied to emergent threat avoidance, i.e. local trajectory planning.

2. UAV trajectory planning modelling.

2.1. UAV models and manoeuvrability constraints. In order to be able to accurately describe the UAV dynamic system, two basic coordinate systems need to be involved namely the Earth inertial coordinate system, and the airframe axis coordinate system [25].

The Earth’s inertial coordinate system is dependent on the Earth being constant with respect to the ground. The OX, OY and OZ axes form a right-handed coordinate system, with the Z axis being the altitude axis. The origin of the coordinate system, O, is the centre of mass of the vehicle.

UAV attitude is often expressed in terms of Euler angles, i.e. yaw angle θ , pitch angle and roll angle γ . In the earth inertial coordinate system, the yaw angle represents the angle between the projection of the longitudinal axis of the body in the OXY plane and the positive direction of the OX axis, the pitch angle represents the angle between the longitudinal axis of the body and the horizontal plane OXY, and the roll angle represents the angle between the number axis of the body and the plumb plane passing through the longitudinal axis OZ of the vehicle.

In solving the route planning problem, the UAV is considered as a mass point and the motion of the UAV at time t can be represented as a vector quantity.

$$X(t) = [x(t), y(t), z(t), \theta(t), \varphi(t)]^T \tag{1}$$

where $x(t), y(t), z(t)$ are the coordinates of the UAV position in the inertial coordinate system, $\theta(t)$ is the UAV yaw angle and $\varphi(t)$ is the UAV pitch angle. For the sake of simplicity, the roll angle is not considered in this paper.

Combined with the kinematics of the mass, the following relationships are available in the Earth’s inertial system.

$$\begin{aligned} \dot{x}(t) &= V \cos \theta(t) \cos \varphi(t), \dot{y}(t) = V \sin \theta(t) \cos \varphi(t) \\ \dot{z}(t) &= V \sin \varphi(t), \dot{\theta}(t) = \eta, \dot{\varphi}(t) = \mu \end{aligned} \tag{2}$$

where η is the control input for the yaw angle of the UAV, μ is the control input for the pitch angle of the UAV and V is the speed of the UAV.

Planning an optimal flightable route for an UAV in a 3D environment must not only satisfy the mission requirements, but also its manoeuvrability performance constraints at the same time. These manoeuvring performance metric constraints need to be combined in the route planning algorithm. The main performance metric constraints that need to be met for the UAV trajectory in the route planning task are the minimum track segment constraint, the maximum range constraint, the minimum flight altitude, the maximum yaw angle and the maximum pitch angle. Let p_i denote the i -th flight track point of the UAV, l_i denote the i -th flight track segment length of the UAV and l_{min} denote the minimum track segment length. The constraint can therefore be expressed as

$$l_i > l_{min}, i = 1, 2, \dots, n \tag{3}$$

The maximum range constraint is caused by the problem of limiting the amount of fuel or the length of flight required by the UAV for the mission. This paper assumes that the UAV flies at a constant speed throughout, so to satisfy the time minimum this translates into a requirement that the length of the trajectory must be less than or equal to the maximum range. The total maximum trajectory length is the sum of the length of each trajectory segment and the maximum range is denoted by l_{max} . The maximum range constraint can be expressed as

$$\sum_{i=1}^n \|l_i\| \leq l_{max}, i = 1, 2, \dots, n \tag{4}$$

Using h_{min} to denote the minimum flight altitude constraint throughout the UAV flight and h_i to denote the flight altitude of the i -th segment of the trajectory, the constraint can be expressed as:

$$h_i \geq h_{min}, i = 1, 2, \dots, n \tag{5}$$

The yaw angle limit is also effectively a minimum turn radius limit. The smaller the turn angle the smoother the UAV can fly. Let the maximum yaw angle allowed for the UAV be θ and the maximum pitch angle be φ , then these two constraints can be expressed as follows respectively.

$$\cos \theta \leq \frac{a_i^T a_{i+1}}{\|a_i\| \|a_{i+1}\|}, i = 2, \dots, n - 1 \tag{6}$$

$$\tan \varphi \geq \frac{|z_i - z_{i-1}|}{|a_i|}, i = 2, \dots, n - 1 \tag{7}$$

The maximum yaw angle constraint is shown in Figure 1. The constraints that are typically used on UAVs are not set in stone, and the UAV will focus on the appropriate constraints for different missions or at different stages of the mission.

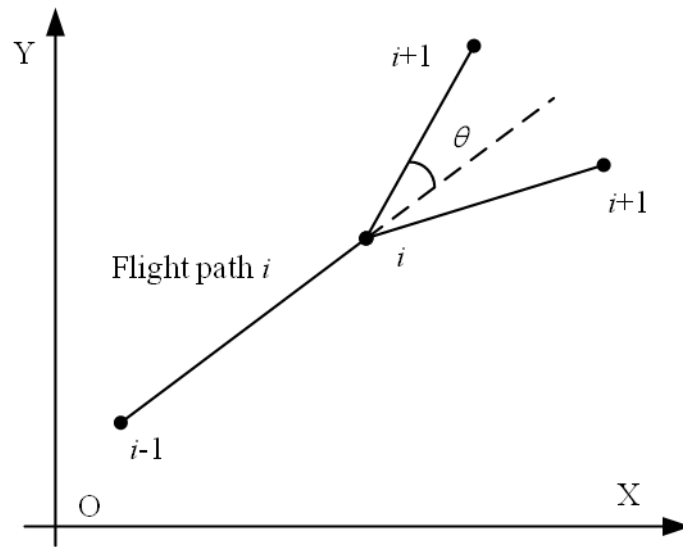


Figure 1. Schematic diagram of the maximum yaw angle constraint

2.2. Construction of equivalent digital maps. A safe UAV flight trajectory requires the UAV to satisfy two conditions when performing its mission, namely terrain following and threat avoidance.

During the flight of the UAV, onboard detection equipment is used to collect and model threat information in the UAV’s surroundings in real time. The new threat information is then fused into an equivalent digital map that is loaded onto a storage device prior to take-off, generating the digital map needed for real-time trajectory planning. This allows for fast access to information for online track planning while transforming threat avoidance into terrain avoidance, thereby simplifying the algorithm’s search processing of map information.

This work uses a functional simulation method to simulate the generation of real terrain.

$$z_1(x, y) = \sin(y + a) + b \cdot \sin(x) + c \cdot \cos \left(d \cdot \sqrt{x^2 + y^2} \right) + e \cdot \cos(y) + f \cdot \sin \left(g \cdot \sqrt{x^2 + y^2} \right) \tag{8}$$

where x and y are the coordinates of the points projected on the horizontal plane by the model, z_1 represents the height value corresponding to the horizontal plane points and a, b, c, d, e, f, g represents the coefficients (which control the base terrain undulations in the digital map).

By determining different constant coefficients to simulate different baseline terrain features as the baseline terrain for the UAV flight environment. The mathematical model for the higher natural hills in the flight environment is described by an exponential function, which can be expressed as

$$z_2(x, y) = \sum_{i=1}^n h_i \exp \left[- \left(\frac{x - x_i}{x_{si}} \right)^2 - \left(\frac{y - y_i}{y_{si}} \right)^2 \right] \quad (9)$$

where (x_i, y_i) is the centre of the i th peak, h_i is the topographic parameter and n is the total number of peaks. x_{si} and y_{si} are the attenuation of the i th peak along the x-axis and y-axis, respectively.

The handling of threats is critical in track planning and if not handled correctly the planned track may have safety issues. The coordinates of the threat centre are assumed to be (x_i, y_i) and the spatial distribution of threat levels is $f_i(x, y)$. A smooth threat distribution model is used in this work.

$$z_3(x, y) = f_i(x, y) = \frac{\alpha_i}{(b_i + c_i(x - x_i)^2 + d_i(y - y_i)^2)^n} \quad (10)$$

The distribution of general static threats [26] can be expressed as

$$f(x, y) = \sum_{i=1}^M f_i(x, y) \quad (11)$$

For the UAV flight space, the environment was modelled using the methods described above and then converted into data that could be processed by a computer, and then an information fusion strategy was used to create an equivalent digital map. The height information of terrain, peaks and threats were fused to obtain an information fusion model $z(x, y)$.

$$z(x, y) = \max(z_1(x, y), z_2(x, y), z_3(x, y)) \quad (12)$$

3. 3D dynamic trajectory planning based on improved A* algorithm and differential evolution.

3.1. Track cost evaluation function. The primary role of the track cost evaluation function is to find the track with the lowest total cost by guiding the track planning algorithm to balance the threat cost and the range cost.

Often in track planning track length and threat cost are in conflict with each other. Since this paper uses a full probability equivalent digital map, the equation for the cost of the trajectory evaluation function in this paper is

$$J = \sum (w_1 * L_i + w_2 * P_i) \quad (13)$$

where P_i is the probability of threat to the i -th track, L_i is the length of the i th track, and w_1 and w_2 are the corresponding weighting factors.

3.2. Improved A* algorithm design. After establishing a fully probabilistic integrated digital map and a track cost evaluation function, this work uses the improved A* algorithm for global track planning design.

A* algorithm is a classical heuristic search algorithm, which is suitable for solving the minimum cost path between two points in the state space and is widely used in path planning [27]. A* algorithm usually searches for the minimum cost track through the set cost function on the basis of gridding the planning environment, and its track cost evaluation function is as follows:

$$f(n) = g(n) + h(n) \quad (14)$$

Where $g(n)$ is the actual cost from the starting point to the current node n , and $h(n)$ is the heuristic function, indicating the cost estimation from the current node to the target point.

A* algorithm adds heuristic function to the flight path cost evaluation function, and does not need to traverse all nodes, which makes the search move faster along the target direction and improves the search efficiency. Firstly, the environment space is divided into a grid space composed of points and edges, and then nodes are expanded from the starting point according to the cost function. Every time the current point is expanded, eight nodes around the current point are taken as sub-nodes to be expanded, and the cost evaluation function value of each sub-node to be expanded is calculated, and the node with the smallest cost evaluation function value is selected as the next search node, so that the search advances in the most favorable direction until the target point is finally reached.

When A* algorithm is applied to the three-dimensional path planning of UAV, its efficiency and accuracy have a certain conflict because of its low delay [28], and it cannot be controlled by effective means to produce better path planning with low delay.

Sparse A* algorithm, based on A* algorithm, effectively reduces the search space and search time by adding constraints of UAV, but there is also the risk of missing the best path. Therefore, it is necessary to further optimize the risk problem to ensure that the route planning can be carried out quickly and the optimal path can be obtained. Because the planned trajectory combines constraints and can meet the maneuverability of UAV, it can be directly applied to UAV flight.

In order to solve the winding path problem of the sparse A* algorithm, an improved sparse A* algorithm is proposed to reduce the winding path of the trajectory by extracting the path feature points and quadratic optimization. Using the principle of continuous function to find the inflection point, the obtained paths are quadratically derived to obtain the set of quadratic derivatives, and then the feature points are selected according to certain selection criteria. As digital maps are used in this paper, the paths are sets of discrete values, so the quadratic derivatives are carried out in the same way as the discrete functions.

(1) Feature points are extracted in the manner shown below.

$$\begin{aligned}\Delta x(n) &= x(n) - x(n-1), n \geq 2 \\ \Delta y(n) &= y(n) - y(n-1), n \geq 2 \\ \Delta \delta &= (|\Delta x(n) - \Delta x(n-1)| + |\Delta y(n) - \Delta y(n-1)|) \geq 10e - 5, n \geq 3\end{aligned}\tag{15}$$

where $x(n)$ and $y(n)$ are the coordinates of node n .

(2) Redundant feature point rejection.

Since there are redundant points in the obtained path feature points, the redundant feature points are eliminated to optimise the path as much as possible. After temporarily eliminating one of the more concentrated path feature points in turn, if the value of the track generation between the two points before and after the eliminated point is less than the value of the track generation of the three points before the elimination, the point needs to be eliminated, otherwise the point cannot be eliminated. Then, the next feature point rejection is performed until there are no feature points left that cannot be rejected. Finally, the optimal feature points are obtained.

(3) Secondary optimisation.

After the optimal path feature points are obtained through feature point rejection, there are cases where the feature points are much larger than the minimum step size due to the redundant feature points being eliminated, so the optimal feature points are optimized

twice to meet the actual flight requirements of the UAV. The distance between adjacent feature points is calculated to be greater than the minimum step size l_{min} . If it is greater than l_{min} , the distance between adjacent feature points is expanded by adding points to the minimum step size until all points meet the constraint.

3.3. Global track planning based on the improved A* algorithm. Since the improved A* algorithm solves the path-winding problem of the sparse A* algorithm, it is applied to the global static pre-trajectory planning of UAVs, as shown in Figure 2.

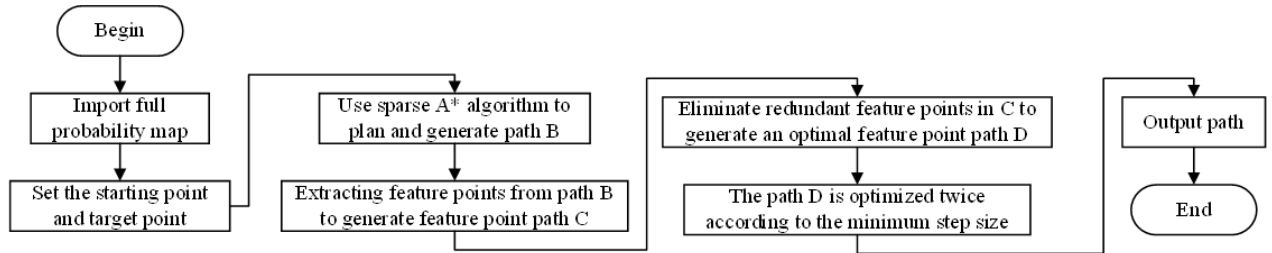


Figure 2. Global track planning based on the improved A* algorithm

3.4. Principle of the Differential Evolutionary Algorithm. The differential evolution algorithm. as a population intelligence optimization algorithm [29], borrows its basic principles from the design philosophy of genetic algorithms.

Compared to genetic algorithms, differential evolution algorithms are more effective and converge faster. Let $X_i(t) (t = 1, 2, \dots, N)$ be the evolved individuals in the current population in the differential evolution algorithm, and the variation operation is performed as follows.

$$V_i(t) = (v_{i1}(t), v_{i2}(t), \dots, v_{iD}(t)) = X_{p1}(t) + F(X_{p2}(t) - X_{p3}(t)) \quad (16)$$

where $X_{pi}(t)$ denotes an individual individual in the population, t denotes the number of current iterations, and F denotes the scaling factor. d is the dimensionality of the individuals in the population.

The crossover operation is performed on different evolved individuals $X_i(t)$ and $V_i(t)$, resulting in a new competing individual $U_i(t) = (u_{i1}(t), u_{i2}(t), \dots, u_{iD}(t))$. The j -th component of the competing individuals $U_i(t)$ is calculated as shown in equation (2).

$$u_{ij}(t) = \begin{cases} v_{ij}(t) & \text{rand}j(0, 1) \leq C_R \text{ or } j \neq z \\ x_{ij}(t) & \text{rand}j(0, 1) > C_R \text{ and } j = z \end{cases} \quad (17)$$

where z denotes a random integer and $z \in \{1, 2, \dots, D\}$. $C_R \in [0, 1]$ denotes the crossover probability.

Comparison of competing individuals with evolved individuals in the current population by fitness values and selection between the two above for merit-based population renewal as follows.

$$X_i(t + 1) = \begin{cases} U_i(t) & \text{IF } f(U_i(t)) \leq f(X_i(t)) \\ X_i(t) & \text{IF } f(U_i(t)) > f(X_i(t)) \end{cases} \quad (18)$$

The pseudo-code for the differential evolution algorithm is shown in Algorithm 1.

Algorithm 1 Differential Evolution

Input: population size M ; crossover factor D ; number of iterations T

Output: a population with optimal adaptation

```

1:  $t \leftarrow 1$ 
2: for  $i = 1$  to  $M$  do
3:   for  $j = 1$  to  $D$  do
4:      $x_{i,t}^j = x_{\min}^j + \text{rand}(0, 1) * (x_{\max}^j - x_{\min}^j)$ ;
5:   end
6: while ( $|f(\Delta)| \geq \varepsilon$ ) or ( $t \leq T$ ) do
7:   for  $i = 1$  to  $M$  do
8:      $\Rightarrow$  (Mutation and Crossover)
9:     for  $j = 1$  to  $D$  do
10:       $v_{i,t}^j = \text{Mutation}(x_{i,t}^j)$ ;
11:       $u_{i,t}^j = \text{Crossover}(x_{i,t}^j, v_{i,t}^j)$ ;
12:     end
13:      $\Rightarrow$  (Selection)
14:     if  $f(u_{i,t}) < f(x_{i,t})$  then
15:        $x_{i,t} \leftarrow u_{i,t}$ ;
16:       if  $f(x_{i,t}) < f(\Delta)$  then
17:          $\Delta \leftarrow x_{i,t}$ ;
18:       end
19:     else
20:        $x_{i,t} \leftarrow x_{i,t}$ ;
21:     end
22:   end
23:    $t = t + 1$ 
24: end
25: return the best  $\Delta$ 

```

3.5. Combination of improved A* algorithm and differential evolution algorithm. The combined dynamic trajectory planning algorithm designed in this work makes full use of the global planning features of the improved A* algorithm and the real-time planning capability of the differential evolution algorithm.

First, the optimal reference trajectory is planned in the entire planning space using the improved A* algorithm. When unknown threat information is detected on the reference trajectory, it enters the local planning phase using the differential evolution algorithm to replan and locally adjust the original reference trajectory to avoid the threat. The flow of the proposed dynamic trajectory planning method is shown in Figure 3.

4. 3-D simulation results and analysis.

4.1. Experimental parameters. In order to verify the effectiveness and applicability of the proposed dynamic route planning combination algorithm, we select wild mountain scenes and urban building scenes for simulation experiments. In order to verify the effectiveness of the algorithm, the combined algorithm is simulated on IntelCorei7-9700K@3.20GHz PC. The running environment is Windows 7's 32-bit operating system with 4.00 GB of memory, and the simulation software is Matlab7.10.0(R2010a).

The starting point and target point of the UAV in the flight area are set, where the coordinates of the starting point S are (2,2,2) and the coordinates of the target point G are (35,20,5). The manoeuvrability limits of the UAV are set as follows: minimum flight height is 40 m; maximum yaw angle is 60°; maximum pitch angle is 30°; maximum range is 1.5 times the straight-line distance between S and G. The parameters of the differential evolution algorithm are set as shown in Table 1.

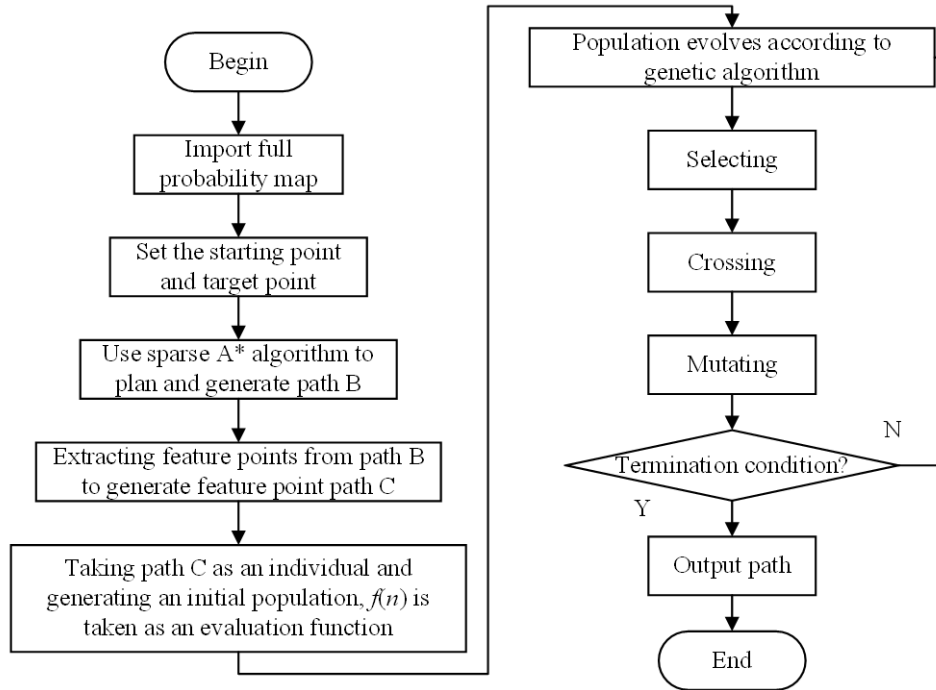


Figure 3. 3D dynamic trajectory planning process based on improved A* and differential evolution

Table 1. Experimental parameters of DE algorithm.

Parameters	Numerical values
Population size	40
Initial scaling factor	0.6
Crossover probabilities C_R	0.2
Dimension D of individuals in the population	20
Error targets ε	0.01
Maximum number of iterations	20,000

4.2. 3D dynamic trajectory planning simulation. In order to be able to fully verify the effectiveness of the proposed combined dynamic trajectory planning algorithm, the simulation experiment was divided into two scenarios, including a mountain peak threat scenario and an urban building complex scenario.

Scene 1: Mountain peak threat scenario. Set the starting point and target point of the UAV in the flight area, where the coordinates of the starting point are (2,2,2) and the coordinates of the target point are (35,20,7). The coordinates of the burst threat are positioned at (32,15). The results of the 3D dynamic trajectory planning are shown in Figures 4, 5, 6 and 7. Among them, Figures 4 and 5 show the 3D dynamic planning results using the sparse A* algorithm, and Figures 6 and 7 show the 3D dynamic planning results using the combined algorithm. The red trajectory is the statically planned reference trajectory and the green trajectory is the secondary replanned (avoidance of emergent threats) safety trajectory after a threat has been detected.

In the early stages of differential evolutionary algorithms there are usually chromosomes with unusually large fitness. These chromosomes have a higher probability of being selected in the population. Although having a high competitive power will control the

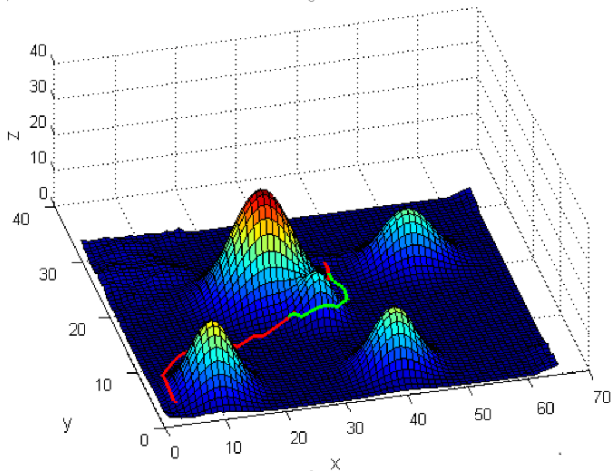


Figure 4. Scene 1 Sparse A*

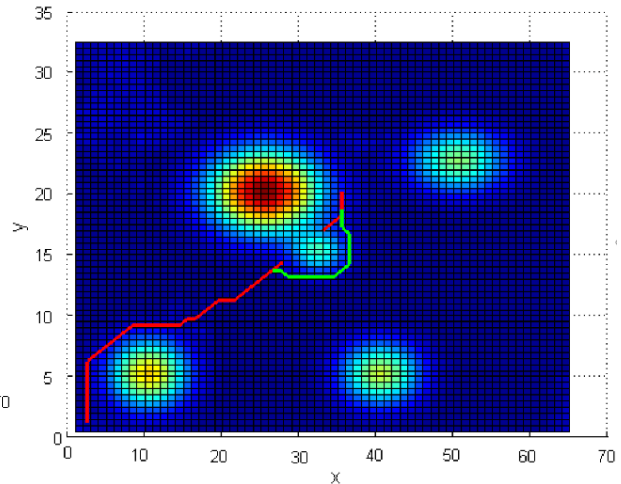


Figure 5. Scene 1 Sparse A*

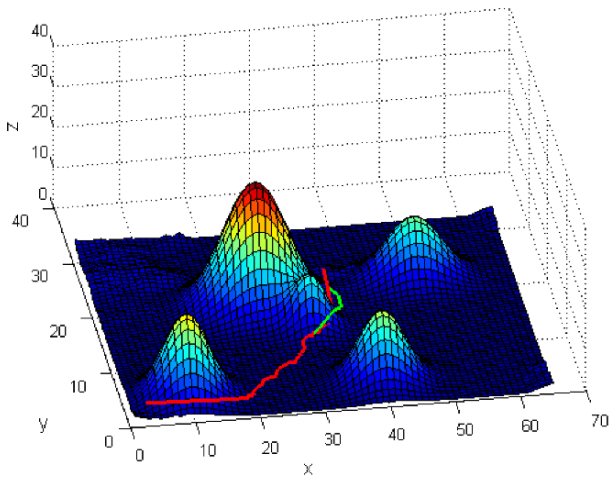


Figure 6. Scenario I Improved A*+DE

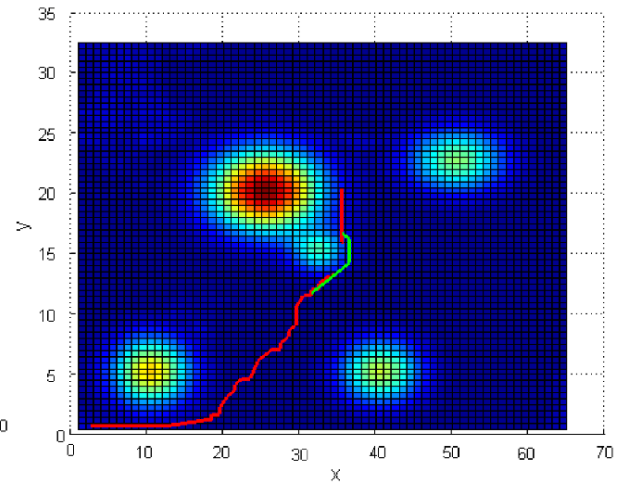


Figure 7. Scenario I Improved A*+DE

selection process, the global search process of the differential evolution algorithm does not appear premature and converges faster.

It can be seen that in the case of an unexpected threat, both planning methods are able to avoid the unexpected threat and quickly replan a new safe trajectory for the UAV, which will return to the original reference trajectory once the UAV reaches the locally planned target point. This is because the improved A* algorithm generates a globally optimal trajectory in the static phase better than the traditional sparse A* algorithm, and the differential evolution algorithm is used in the replanning phase to quickly plan a trajectory that avoids emergent threats.

Scenario 2: Urban threat scenario. Set the coordinates of the start point to (3,3,3) and the coordinates of the target point to (45,23,5). Assume the coordinate position of the new no-fly zone during the flight is (40,15). The results of the 3D dynamic trajectory planning are shown in Figures 9, 9, 10 and 11. Among them, Figures 8 and 9 show the 3D dynamic planning results using the sparse A* algorithm, and Figures 10 and 11 show the 3D dynamic planning results using the combined algorithm.

The comparison shows that the trajectory of Figure 11 is better. The simulation plots show that in the environment of dense urban buildings, the combination of the improved

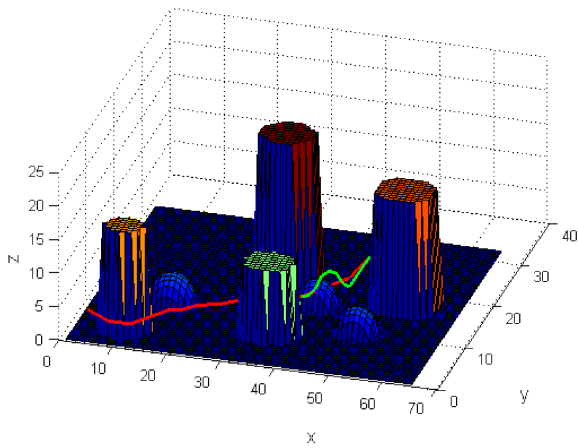


Figure 8. Scene II Sparse A*

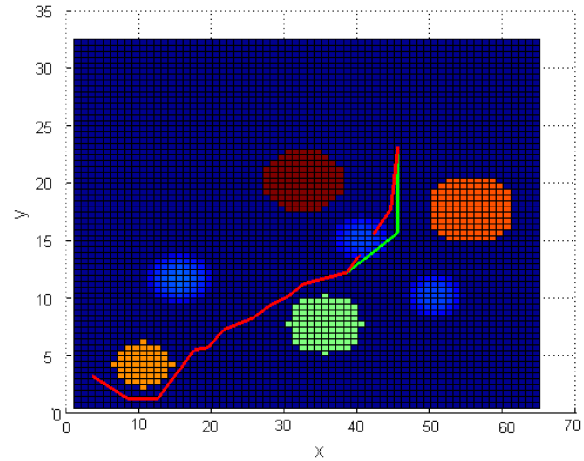


Figure 9. Scene II Sparse A*

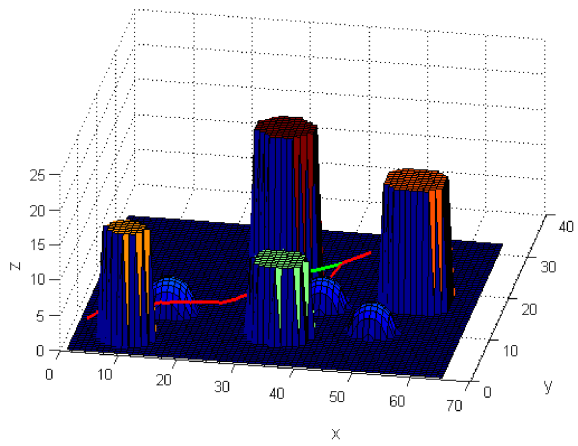


Figure 10. Scenario II Improved A*+DE

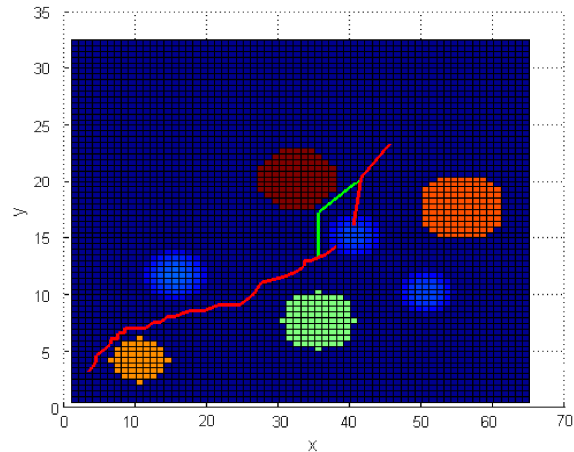


Figure 11. Scenario II Improved A*+DE

sparse A* and differential evolution algorithm is still able to achieve real-time UAV trajectory planning, avoiding tall buildings and no-fly zones, verifying the feasibility and effectiveness of the algorithm proposed in this paper.

Table 2 shows the over-all properties comparison. From the experimental data, it can be seen that compared with the basic sparse A* algorithm, although the combined algorithm reduces the convergence speed, the planned path is shorter, the total cost is smaller, and the performance of the algorithm is improved.

Table 2. The overall properties comparison

Algorithms	Convergence speed/s	Path length/km	Overall cost
Sparse A* algorithm	21.97	197.67	247.39
Improved A*+DE	22.78	156.52	201.44

5. Conclusion. This work proposes a method that uses a combination of an improved A* algorithm and a differential evolutionary algorithm, applied to 3D trajectory planning in complex environments. The mathematical modelling of the problems related to UAV

track planning, including the UAV model, manoeuvrability constraints and equivalent digital maps, is performed. An improved sparse A* algorithm is proposed for solving the winding path problem of the sparse A* algorithm, which reduces the winding path of the trajectory by extracting path feature points and quadratic optimisation. The improved sparse A* is combined with the differential evolutionary algorithm and applied to UAV real-time track planning, where the improved sparse A* algorithm is used for UAV global track planning, while the differential evolutionary algorithm is applied to emergent threat avoidance, i.e. local track planning. Simulation results show that the combined algorithm results in shorter path distances and a smaller total cost than the sparse A* algorithm. Subsequent research will use real UAVs in real outdoor scenarios for validation of effectiveness and consider more physical condition constraints for more accurate calculation of the total cost of the trajectory.

Acknowledgement. This work is partially supported by sichuan research center of higher vocational education (No. GZY22C21), and national industrial and information technology vocational education and teaching steering committee (No. GXHZWC15750).

REFERENCES

- [1] S. Liu, and C.-M. Chen, "Comments on "A Secure and Lightweight Drones-Access Protocol for Smart City Surveillance", " *IEEE Transactions on Intelligent Transportation Systems*, vol. 23, no. 12, pp. 25054-25058, 2022.
- [2] T. Wu, X. Guo, Y. Chen, S. Kumari, and C. Chen, "Amassing the Security: An Enhanced Authentication Protocol for Drone Communications over 5G Networks," *Drones*, vol. 6, no. 1, 10, 2021.
- [3] M. A. Khan, I. Ullah, M. H. Alsharif, A. H. Alghtani, A. A. Aly, and C.-M. Chen, "An Efficient Certificate-Based Aggregate Signature Scheme for Internet of Drones," *Security and Communication Networks*, vol. 2022, pp. 1-9, 2022.
- [4] S. C. Kakarla and Y. Ampatzidis, "Postflight Data Processing Instructions on the Use of Unmanned Aerial Vehicles (UAVs) for Agricultural Applications," *EDIS*, vol. 2019, no. 6, pp. 6-15, 2019.
- [5] I. Elkharchy, "Accuracy Assessment of Low-Cost Unmanned Aerial Vehicle (UAV) Photogrammetry," *Alexandria Engineering Journal*, vol. 60, no. 6, pp. 5579-5590, 2021.
- [6] N. Elmeseiry, N. Alshaer, and T. Ismail, "A Detailed Survey and Future Directions of Unmanned Aerial Vehicles (UAVs) with Potential Applications," *Aerospace*, vol. 8, no. 12, 363, 2021.
- [7] T.-Y. Wu, A. Shao, and J.-S. Pan, "CTOA: Toward a Chaotic-Based Tumbleweed Optimization Algorithm," *Mathematics*, vol. 11, no. 10, 2339, 2023.
- [8] T.-Y. Wu, H. Li, and S.-C. Chu, "CPPE: An Improved Phasmatodea Population Evolution Algorithm with Chaotic Maps," *Mathematics*, vol. 11, no. 9, 1977, 2023.
- [9] N. A. Khan, N. Z. Jhanjhi, S. N. Brohi, R. S. A. Usmani, and A. Nayyar, "Smart traffic monitoring system using Unmanned Aerial Vehicles (UAVs)," *Computer Communications*, vol. 157, pp. 434-443, 2020.
- [10] C. Qu, W. Gai, J. Zhang, and M. Zhong, "A novel hybrid grey wolf optimizer algorithm for unmanned aerial vehicle (UAV) path planning," *Knowledge-Based Systems*, vol. 194, p105530, 2020.
- [11] E. V. Butilă and R. G. Boboc, "Urban Traffic Monitoring and Analysis Using Unmanned Aerial Vehicles (UAVs): A Systematic Literature Review," *Remote Sensing*, vol. 14, no. 3, 620, 2022.
- [12] M. Shah Alam and J. Oluoch, "A survey of safe landing zone detection techniques for autonomous unmanned aerial vehicles (UAVs)," *Expert Systems with Applications*, vol. 179, 115091, 2021.
- [13] G. Jang, J. Kim, J.-K. Yu, H.-J. Kim, and Y. Kim, "Review: Cost-Effective Unmanned Aerial Vehicle (UAV) Platform for Field Plant Breeding Application," *Remote Sensing*, vol. 12, no. 6, 998, 2020.
- [14] G. Wang, Y. Han, X. Li, J. Andaloro, and P. Chen, "Field evaluation of spray drift and environmental impact using an agricultural unmanned aerial vehicle (UAV) sprayer," *Science of The Total Environment*, vol. 737, 139793, 2020.
- [15] C. Doughty and K. Cavanaugh, "Mapping Coastal Wetland Biomass from High Resolution Unmanned Aerial Vehicle (UAV) Imagery," *Remote Sensing*, vol. 11, no. 5, p. 540, Mar. 2019.

- [16] C. Qu, W. Gai, M. Zhong, and J. Zhang, "A novel reinforcement learning based grey wolf optimizer algorithm for unmanned aerial vehicles (UAVs) path planning," *Applied Soft Computing*, vol. 89, 106099, 2020.
- [17] H. Chen, Y. Lan, B. K. Fritz, W. Clint Hoffmann, and S. Liu, "Review of agricultural spraying technologies for plant protection using unmanned aerial vehicle (UAV)," *International Journal of Agricultural and Biological Engineering*, vol. 14, no. 1, pp. 38-49, 2021.
- [18] J. A. Guerrero and Y. Bestaoui, "UAV Path Planning for Structure Inspection in Windy Environments," *Journal of Intelligent & Robotic Systems*, vol. 69, no. 1, pp. 297-311, 2012.
- [19] J. da Silva Arantes, M. da Silva Arantes, C. F. Motta Toledo, O. T. Júnior, and B. C. Williams, "Heuristic and Genetic Algorithm Approaches for UAV Path Planning under Critical Situation," *International Journal on Artificial Intelligence Tools*, vol. 26, no. 1, 1760008, 2017.
- [20] C. Huang and J. Y. Fei, "UAV Path Planning Based on Particle Swarm Optimization with Global Best Path Competition," *International Journal of Pattern Recognition and Artificial Intelligence*, vol. 32, no. 6, 1859008, 2018.
- [21] A. Majeed and S. O. Hwang, "Path Planning Method for UAVs Based on Constrained Polygonal Space and an Extremely Sparse Waypoint Graph," *Applied Sciences*, vol. 11, no. 12, 5340, 2021.
- [22] Y. Chen, G. Luo, Y. Mei, J. Yu, and X. Su, "UAV path planning using artificial potential field method updated by optimal control theory," *International Journal of Systems Science*, vol. 47, no. 6, pp. 1407-1420, 2014.
- [23] N. Bolourian and A. Hammad, "LiDAR-equipped UAV path planning considering potential locations of defects for bridge inspection," *Automation in Construction*, vol. 117, 103250, 2020.
- [24] H. M. Jayaweera and S. Hanoun, "A Dynamic Artificial Potential Field (D-APF) UAV Path Planning Technique for Following Ground Moving Targets," *IEEE Access*, vol. 8, pp. 192760-192776, 2020.
- [25] V. Jamshidi, V. Nekoukar, and M. H. Refan, "Real time UAV path planning by parallel grey wolf optimization with align coefficient on CAN bus," *Cluster Computing*, vol. 24, no. 3, pp. 2495-2509, 2021.
- [26] Q. Liu, L. Shi, L. Sun, J. Li, M. Ding, and F. S. Shu, "Path Planning for UAV-Mounted Mobile Edge Computing with Deep Reinforcement Learning," *IEEE Transactions on Vehicular Technology*, vol. 69, no. 5, pp. 5723-5728, 2020.
- [27] L. Zhang, Z.-J. Qiao, M.-D. Xing, J.-L. Sheng, R. Guo, and Z. Bao, "High-Resolution ISAR Imaging by Exploiting Sparse Apertures," *IEEE Transactions on Antennas and Propagation*, vol. 60, no. 2, pp. 997-1008, 2012.
- [28] Z. Zhang, J. Wu, J. Dai, and C. He, "Rapid Penetration Path Planning Method for Stealth UAV in Complex Environment with BB Threats," *International Journal of Aerospace Engineering*, vol. 2020, pp. 1-15, 2020.
- [29] Y. Zhang, D. Gong, X. Gao, T. Tian, and X. Sun, "Binary differential evolution with self-learning for multi-objective feature selection," *Information Sciences*, vol. 507, pp. 67-85, 2020.